Preliminary Design of an Axial-Flow Compressor

OSPINO R, JUAN D.[1] AND ABAUNZA M, ÓSCAR A.[1]

[1] *Aerospace Engineering. Mechanical and Aerospace Department. Universidad de Antioquia. Medellín*

Date May 10, 2024

This study focuses on the preliminary design of an axial flow compressor, blending theoretical analysis with Computational Fluid Dynamics (CFD) simulations. The methodology begins with a thorough examination of fundamental concepts and theories related to axial flow compressors, followed by the identification of key parameters for defining compressor geometry. After establishing mathematical solutions, a 3D model is created. Using this information, a mesh is implemented to enable effective simulation of the compressor's behavior in Ansys CFX, facilitating the analysis of results.

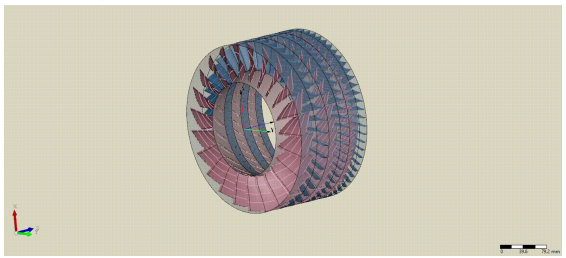

Fig. 1. Axial-flow compressor created with CF - Turbo

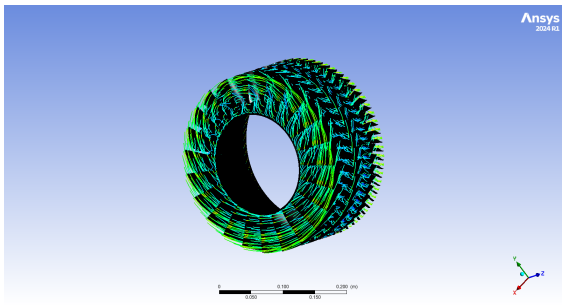

Fig. 2. Axial-flow compressor simulated with ansys - CFX

1. INTRODUCTION

Turbomachinery is central to the functioning of gas turbine engines. The compressor plays a critical role in mechanical air compression within the engine, with the shaft power to operate the compressor typically being generated by expanding gases in the turbine. Turbomachinery encompasses machines that exchange energy with a working fluid through shaft rotation. When the fluid path aligns predominantly with the axis of shaft rotation, these machines are classified as axial-flow turbomachinery. Axial-flow compressors and turbines are extensively used and developed in aircraft gas turbine engines [1].

Given the significant importance of axial-flow compressors in aircraft, this study explores the implementation of a design process for this type of turbomachinery. The aim is to develop a 3D simulated model that demonstrates both thermodynamic and aerodynamic performance based on a series of numerical solutions. This research follows the comprehensive design process outlined in the book "Gas Turbine Theory, 7th Edition, Chapter 5, Subsection 5.7: Design Process" by G. F. C. Rogers, H. I. H. Saravanamuttoo, and Henry Cohen [2].

After obtaining the numerical results, the study focuses on generating the geometry. At this stage, engineering software such as CFTurbo and Ansys Workbench were utilized. The goal is to align the theoretical data with the parameters controlling the geometry within the software. Once this process is successfully completed, a validation step is undertaken by simulating the 3D model. The study includes a comparison between numerical and simulated results at this point.

2. DESIGN PROCESS

The research aims to present readers with a preliminary design. The proposed methodology is outlined as follows:

A. Theoretical Approach

The complete design process for the compressor will encompass the following steps:

1. choice of design point;
2. determination of rotational speed and annulus dimensions;
3. determination of number of stages, using an assumed efficiency;
4. calculation of the air angles for each stage at the mean radius;
5. determination of the variation of the air angles from root to tip;

6. investigation of compressibility effects;
7. selection of compressor blading, using experimentally obtained cascade data;
8. check on efficiency previously assumed, using the cascade data;
9. estimation of off-design performance;
10. rig testing.

See [1, 2].

By focusing on the most fundamental parameters for an initial yet robust design run, it was determined that the first four steps encapsulate the key aspects of a preliminary design.

The design point under sea-level static conditions ($P_a = 101$ kPa and $T_a = 288$ K) may be identified as:

→ Compressor pressure ratio: 5.22

→ Air mass flow: 10.3 kg/s

A.1. Determination of rotational speed and annulus dimensions

This can be found by assuming values for the blade tip speed, the axial velocity and hub–tip ratio at the inlet to the first stage. The required annulus area at entry is obtained from the specified mass flow, axial velocity, and ambient conditions.

Assuming ideal conditions with no intake loss nor pre-whirled flow (without Inlet Guide Vanes), the axial velocity remains constant throughout the compressor ($C_{a1} = 150\,\mathrm{m/s}$). Considering standard and acceptable values for tip speed (U_t) at 350 m/s and allowing for hub-to-tip ratio variations between 0.4 and 0.6 to ensure acceptable stresses, a framework is established. Additionally, under the assumption of air behaving as an ideal gas ($R = 0.287\,\mathrm{kJ/kgK}$; $C_p = 1.005\,\mathrm{kJ/kgK}$; $\gamma = 1.4$), the static thermodynamic conditions at the inlet can be determined. This, in turn, enables the ascertainment of the rotational speed and annulus dimensions.

The governing equation are shown bellow:

$$\dot{m} = \rho_1 A C_{a1} = \rho_1 \pi r_t^2 \left[1 - \left(\frac{r_r}{r_t}\right)^2\right]$$

$$r_t^2 = \frac{\dot{m}}{\pi \rho_1 C_{a1}[1 - (r_r/r_r)^2]}$$

$$T_1 = T_a - \frac{C_{a1}^2}{2C_p \times 10^3}$$

$$P_1 = P_a \left[\frac{T_1}{T_a}\right]^{\gamma/(\gamma-1)}$$

$$\rho_1 = \frac{P_1}{RT_1}$$

Finally, it can determine the rotational speed as:

$$N = \frac{U_t}{2\pi r_t}$$

Evaluating r_t and N over the range of hub-to-tip ratio, leads the values expressed in Table 1.

Considering a conservative value for $r_r/r_t = 0.5$, the rotational speed reaches approximately $N \approx 20600$ RPM and $r_t = 0.1623$ m.

Adjusting this selection yields the current value for tip speed:

Table 1. Variation of r_t and N

r_r/r_t	r_t [m]	N [rev/s]	N [RPM]
0.40	0.1533	363.2720	21796.3224
0.45	0.1574	353.9628	21237.7707
0.50	0.1623	343.2598	20595.5888
0.55	0.1683	331.0278	19861.6666
0.60	0.1757	317.0898	19025.3900

$$U_t = 2\pi r_t N \approx 350\ \mathrm{m/s}$$

Reader can noticed the value for tip speed keeps under the range from 450 to 550 m/s for real turbofan compressor turbomachinery [1].

Another important consideration is the Mach number at the inlet of the first stage:

$$V_{1t}^2 = U_{1t}^2 + C_{a1}^2$$

$$a = \sqrt{(\gamma R T_1)}$$

$$M_{1t} = \frac{V_{1t}}{a}$$

The preceding calculations result in a relative speed of $V_{1t} = 380.9$ m/s, a speed of sound of $a = 333.5$ m/s, and a Mach number of $M_{1t} = 1.1$.

The earlier calculations indicate that at the inlet, the compressor operates within the transonic regime. However, this Mach number level shouldn't pose any issues; in fact, it's quite typical [1–3].

At this stage, the thermodynamic conditions at the inlet have been established, and attention now shifts to the exit conditions. To estimate the compressor delivery temperature, a polytropic efficiency of 0.90 for the compressor will be assumed.

$$T_{02} = T_{01}\left[\frac{P_{02}}{P_{01}}\right]^{(n-1)/n}$$

Where, $\frac{(n-1)}{n} = \frac{1}{0.90} \times \frac{0.4}{1.4} = 0.3175$

$$T_2 = T_{02} - \frac{C_{a2}^2}{2C_p \times 10^3}$$

$$P_2 = P_{02}\left[\frac{T_2}{T_{02}}\right]^{\gamma/(\gamma-1)}$$

$$\rho_2 = \frac{P_2}{RT_2}$$

$$A_2 = \frac{\dot{m}}{\rho_2 \times C_{a2}}$$

$$r_m = \frac{r_h + r_t}{2}$$

$$h = \frac{A_2}{2\pi r_m}$$

And the radii at exit is given by:

$$r_t = r_m + (h/2)$$

$$r_t = r_m - (h/2)$$

Tables 2 and 3 summarizes the previous analysis with results.

Table 2. Inlet and Exit Static Conditions

Parameter	Inlet	Exit
Inlet Temperature (K)	276.8	475.5
Inlet Pressure (kPa)	87.9	486.0
Inlet Density (kg/m^3)	1.1066	3.5614
Inlet Axial Velocity (m/s)	150	150

Table 3. Exit Annulus Dimensions

Parameter	Value
Pitchline radius r_m (m)	0.1217
Exit area A_2 (m^2)	0.0193
Blade height at exit h (m)	0.0252
Exit tip radius r_t (m)	0.1343
Exit hub radius r_r (m)	0.1091

A.2. Estimation of number of stages

The overall stagnation temperature rise trough the compressor is $\Delta T_{0C} = 486.7 - 288.0 = 198.7$ K

And the temperature rise across each stage is given by:

$$\Delta T_{0S} = \frac{\lambda U C_a (tan\beta_1 - tan\beta_2)}{C_p}$$

With a purely axial velocity,

$$tan\beta_1 = \frac{U}{Ca}$$

$$V_1 = \frac{Ca}{cos\beta_1}$$

Utilizing the de Haller Criterion of $V_2/V_1 \not< 0.72$

$$V_2 = V_1 \times 0.72$$

This allows to express

$$cos\beta_2 = \frac{C_a}{V_2}$$

Initially disregarding the work-done factor (λ), the calculation yields $\Delta T_{0S} = 27.4$ K. Consequently, this value dictates the number of stages required to achieve the desired outcome.

$$\#Stages = \Delta T_{0C}/\Delta T_{0S} = 8$$

However, factoring in the influence of the work-done factor, it becomes apparent that an appropriate number of stages is 9.

A.3. Stage by stage design

Having determined the rotational speed and annulus dimensions, and estimated the number of stages required, the next step is to evaluate the air angles for each stage at the **mean radius**.

The mean blade speed is $U_m = 2\pi r_m N \approx 262.5$ m/s

The work-done factors will vary through the compressor, and reasonable values for stages would be 0.98 for the first stage, 0.93 for the second, 0.88 for the third and 0.83 for the remaining stages [2, 3].

The governing equations are extensively outlined in [2]. To facilitate an iterative process, a Python script was developed. This script encapsulates the methodology described below:

1. **Iteration:** The code iterates over each stage of the compressor.
2. **Calculations:** Inside each stage iteration, the following calculations are performed:
   - Calculation of the change in tangential velocity (ΔC_w) based on temperature rise (ΔT_0).
   - Calculation of angles (β and α) using trigonometric functions and given velocities.
   - Deflection calculations for rotor blades.
   - Checks for validity based on the de Haller criterion.
   - Calculation of pressure and temperature ratios.
3. **Conditions Handling:** The code handles different conditions based on the stage number.

A pseudo-code is provided for readers to understand the process. Check Algorithm 1.

The outputs of the preceding procedure are presented in Table 4:

A.4. Variation of air angles from root to tip

The governing equations pertinent to this stage of the design are comprehensively elucidated in [2, 3]. However, for a broader understanding of the calculation process, refer to Algorithm 2.

Results of the complete implementation of the respective process is shown in Tables 5, 6, 7, 8.

B. Simulation

In this phase, specialized software tools were utilized to generate the detailed geometry of the compressor. For this purpose, CF-turbo software was chosen, enabling the creation of an accurate 3D model for use in subsequent simulations.

The primary objective for this phase was to focus solely on the first three stages of the compressor's theoretical design. This choice is substantiated by the critical role these initial stages play in axial-flow compressors, typically encompassing the first and last three stages [4, 5]. Additionally, an enhanced design approach was implemented by maintaining a constant outer radius. This decision aligns with the rationale expressed in [2]: "Constant outer diameter compressors are utilized when the minimum number of stages is required, commonly seen in aircraft engines." This justification supports the decision to opt for three stages instead of the entire nine. Moreover, the treatment of air as an ideal gas further simplifies the analysis and enhances the relevance of the simulations.

A graphical depiction of the geometry is provided in Figure 3.

Table 4. Stage Results at Mean Radius

Stage	β_1 (deg)	β_2 (deg)	α_1 (deg)	α_2 (deg)	α_3 (deg)	$\Delta\beta$ (deg)	$Cw1$ (m/s)	$Cw2$ (m/s)	ΔCw (m/s)	λ	ΔT_{05}	P_{03}/P_{01}	P_{03} (KPa)	T_{03} (K)	°R	DeHaller Criterion (Rotor)	DeHaller Criterion (Stator)
1	60.2584	50.8750	0.0000	27.5117	11.8320	9.3833	0.0000	78.1238	78.1238	0.9800	20.0000	1.2364	124.8742	308.0000	0.8512	0.7862	0.7862
2	57.0148	42.2892	11.8320	40.0519	28.4404	14.7256	31.4240	126.0967	94.6726	0.9300	23.0000	1.2557	156.7993	331.0000	0.7000	0.7359	0.7359
3	50.3960	28.4404	28.4404	50.3960	28.2310	21.9556	81.2414	181.2931	100.0518	0.8800	23.0000	1.2365	193.8873	354.0000	0.5000	0.7250	0.7250
4	50.5056	28.2310	28.2310	50.5056	28.2310	22.2746	80.5338	182.0007	101.4669	0.8300	22.0000	1.2098	234.5717	376.0000	0.5000	0.7219	0.7219
5	50.5056	28.2310	28.2310	50.5056	28.2310	22.2746	80.5338	182.0007	101.4669	0.8300	22.0000	1.1968	280.7265	398.0000	0.5000	0.7219	0.7219
6	50.5056	28.2310	28.2310	50.5056	28.2310	22.2746	80.5338	182.0007	101.4669	0.8300	22.0000	1.1852	332.7225	420.0000	0.5000	0.7219	0.7219
7	50.5056	28.2310	28.2310	50.5056	12.0815	22.2746	80.5338	182.0007	101.4669	0.8300	22.0000	1.1750	390.9335	442.0000	0.5000	0.7219	0.7219
8	50.5056	28.2310	28.2310	50.5056	28.9104	22.2746	80.5338	182.0007	101.4669	0.8300	22.0000	1.1658	455.7364	464.0000	0.5000	0.7219	0.7219
9	50.1466	28.9104	28.9104	50.1466	0.0000	21.2362	82.8399	179.6946	96.8547	0.8300	21.0000	1.1569	527.2200	485.0000	0.5000	0.7321	0.7321

Table 5. Geometry Calculations

Stage	Constant Mean radius (m)	Rotor inlet hub radius (m)	Rotor inlet tip radius (m)	Rotor outlet hub radius (m)	Rotor outlet tip radius (m)	Stator outlet hub radius (m)	Stator outlet tip radius (m)	Exit Area (m^2)	Stator Blade Height (m)
1	0.1217	0.0811	0.1623	0.0839	0.1595	0.0867	0.1567	0.0535	0.0700
2	0.1217	0.0867	0.1567	0.0890	0.1544	0.0913	0.1521	0.0465	0.0608
3	0.1217	0.0913	0.1521	0.0934	0.1500	0.0956	0.1478	0.0399	0.0522
4	0.1217	0.0956	0.1478	0.0973	0.1461	0.0989	0.1445	0.0348	0.0456
5	0.1217	0.0989	0.1445	0.1003	0.1431	0.1017	0.1417	0.0306	0.0401
6	0.1217	0.1017	0.1417	0.1028	0.1406	0.1039	0.1395	0.0271	0.0355
7	0.1217	0.1039	0.1395	0.1049	0.1385	0.1059	0.1375	0.0242	0.0317
8	0.1217	0.1059	0.1375	0.1067	0.1367	0.1075	0.1359	0.0217	0.0284
9	0.1217	0.1075	0.1359	0.1083	0.1351	0.1091	0.1343	0.0192	0.0251

Table 6. Blade Speed Calculations

Stage	Mean blade speed (m/s)	Rotor inlet hub blade speed (m/s)	Rotor inlet tip blade speed (m/s)	Rotor outlet hub blade speed (m/s)	Rotor outlet tip blade speed (m/s)	Rotor outlet mean relative speed (m/s)	Rotor outlet hub relative speed (m/s)	Rotor outlet tip relative speed (m/s)	Stage outlet speed [C3] (m/s)
1	262.5345	174.9511	350.1179	180.9799	344.0891	78.1238	113.3286	59.6072	153.2562
2	262.5345	187.0088	338.0603	191.9594	333.1097	126.0967	129.4797	74.6146	170.5877
3	262.5345	196.9100	328.1591	201.5642	323.5048	181.2931	130.3160	81.1952	170.2519
4	262.5345	206.2184	318.8506	209.8087	315.2604	182.0007	126.9659	84.4970	170.2519
5	262.5345	213.3989	311.6701	216.3563	308.7127	182.0007	123.1235	86.2891	170.2519
6	262.5345	219.3137	305.7553	221.7774	303.2916	182.0007	120.1139	87.8315	170.2519
7	262.5345	224.2411	300.8280	226.3141	298.7549	182.0007	117.7061	89.1652	170.2519
8	262.5345	228.3872	296.6818	230.1313	294.9377	182.0007	115.7537	90.3192	171.3547
9	262.5345	231.8754	293.1936	233.6501	291.4190	179.6946	108.8282	87.2548	150.0000

Table 7. Angles Calculations

Stage	β_1 mean (deg)	β_1 hub (deg)	β_1 tip (deg)	β_2 mean (deg)	β_2 hub (deg)	β_2 tip (deg)	Mean Blade Deflection (deg)	Hub Blade Deflection (deg)	Tip Blade Deflection (deg)	α_2 mean (deg)	α_2 hub (deg)	α_2 tip (deg)
1	60.2584	49.3908	66.8084	50.8750	24.2758	62.1985	9.3833	25.1150	4.6099	27.5117	37.0719	21.6720
2	60.2584	51.2668	66.0728	42.2892	22.6132	59.8742	14.7256	28.6536	6.1986	40.0519	40.8007	26.4472
3	60.2584	52.7010	65.4351	28.4404	25.4072	58.2407	21.9556	27.2938	7.1944	50.3960	40.9832	28.4267
4	60.2584	53.9685	64.8058	28.2310	28.9112	56.9755	22.2746	25.0572	7.8304	50.5056	40.2459	29.3931
5	60.2584	54.8963	64.2995	28.2310	31.8631	56.0047	22.2746	23.0332	8.2948	50.5056	39.3800	29.9101
6	60.2584	55.6298	63.8680	28.2310	34.1277	55.1550	22.2746	21.5020	8.7130	50.5056	38.6863	30.3508
7	60.2584	56.2205	63.4981	28.2310	35.9066	54.4093	22.2746	20.3140	9.0888	50.5056	38.1215	30.7287
8	60.2584	56.7039	63.1792	28.2310	37.3261	53.7559	22.2746	19.3778	9.4233	50.5056	37.6571	31.0533
9	60.2584	57.1012	62.9054	28.9104	39.7654	53.6952	21.2362	17.3358	9.2102	50.1466	35.9617	30.1865

Table 8. Thermodynamics Exit Calculations

Stage	Total Exit Temperature (K)	Static Exit Temperature (K)	Total Exit Pressure (kPa)	Static Exit Pressure (kPa)	Exit Density (kg/m^3)	Hub Degree of Reaction
1	308.0000	296.3147	124.8742	109.0640	1.2825	0.6869
2	331.0000	316.5223	156.7993	134.0792	1.4760	0.6627
3	354.0000	339.5793	193.8873	167.6224	1.7199	0.6767
4	376.0000	361.5793	234.5717	204.5645	1.9713	0.6974
5	398.0000	383.5793	280.7265	246.7093	2.2410	0.7155
6	420.0000	405.5793	332.7225	294.4250	2.5294	0.7292
7	442.0000	427.5793	390.9335	348.0833	2.8365	0.7399
8	464.0000	449.3918	455.7364	407.4636	3.1592	0.7485
9	485.0000	473.8060	527.2200	485.8449	3.5729	0.7671

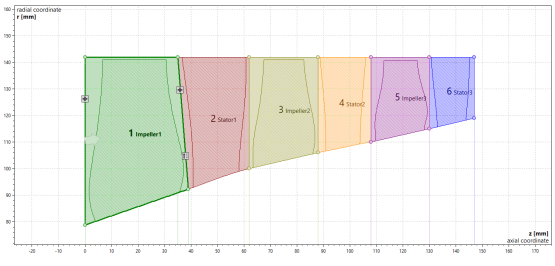

Fig. 3. Final design schematic

Subsequently, the advanced simulation software CFX by Ansys was used to analyze the compressor's performance under various operating conditions. In this analysis, only the RPM values were varied within the previously calculated design operating ranges, utilizing values of 5000, 10000, and 20600 RPM. These simulations allowed for the evaluation of the compressor's behavior, including factors such as pressure, temperature, Mach number, and flow velocity.

The results obtained provide an in-depth understanding of the compressor's performance, facilitating the optimization of its design and ensuring its efficient operation in practical applications.

3. RESULTS AND CONCLUSIONS

In Section B of Appendix, reader can find the plots of the simulations.

A. Mach number

The presence of higher Mach numbers, particularly in small areas of the compressor profile, indicates that certain sections may approach or exceed sonic conditions at higher RPMs.

Another crucial observation pertains to the behavior of velocity vector fields. At 5000 and 10000 RPM (See Figures 4a and 4d), there is a notable increase in velocity at the interface between the rotor and stator. This signifies a loss of efficiency and raises potential risk scenarios such as stall and/or surge. Conversely, at 20600 RPM (Figure 4g), the velocity enhances the blade airfoil, resulting in a more favorable aerodynamic performance with a consistent magnitude flow over the airfoil's surface. Given the unique characteristics observed in the third stage, it is advisable to undertake a complete redesign of this stage to address the observed anomalies effectively.

Furthermore, future research endeavors could explore compressibility effects to gain a more comprehensive understanding of the system's behavior.

B. Temperature

Between 5000 and 10000 RPM (Figures 4b and 4e), the total temperature remains relatively constant throughout the compressor, resulting in a negligible increase in temperature. Consequently, this leads to a low compressor pressure ratio, indicative of suboptimal performance within this RPM range. However, at 12600 RPM (Figure 4h), a discernible increase in temperature is observed in each stage, with the temperature remaining constant within each stage until the interface with another stage. This indicates a favorable design scenario, where the pressure ratio behaves as anticipated, resulting in normal performance.

C. Pressure

These plots vividly illustrate the fluid's behavior, allowing readers to easily discern vortex formations at the leading edge of the rotor blades, particularly evident in the second and third stages, especially at 5000 and 10000 RPM (Figures 4c, 4f). This observation leads to the conclusion that these regimes exhibit sub-optimal performance, underscoring the reliability of theoretical models.

Examining the behavior at 20600 RPM (Figure 4i), vortex formations are minimized. However, at the interface between the second and third stages, the air experiences expansion, resulting in a decrease in pressure. This divergence underscores the need for a redesign of the third stage, as evidenced by the noticeable difference in airfoil shapes between the first two stages and the third stage.

REFERENCES

1. S. Farokhi, *Aircraft Propulsion* (Wiley, 2009).
2. G. F. C. Rogers, H. I. H. Saravanamuttoo, and Henry Cohen, *Gas Turbine Theory* (Pearson College, 2017).
3. A. F. El-Sayed, *Aircraft Propulsion and Gas Turbine Engines* (CRC Press, 2017).
4. N. A. Cumpsty, *Compressor Aerodynamics* (Longman, 2004).
5. S. L. Dixon and C. A. Hall, *Fluid Mechanics and Thermodynamics of Turbomachinery* (Butterworth-Heinemann, 2013).

A. ALGORITHMS

Algorithm 1. Compressor Stage Calculation at Pitchline

Initialize constants: λ, ΔT_{0S}, C_p, U, C_a, e_{pol}, γ_{air}
Initialize arrays: β_1, β_2, α_1, α_2, α_3, $\Delta\beta$, $Cw1$, $Cw2$, ΔCw, P_{03}/P_{01}, P_{03}, T_{03}, $deHallerCriterion_R$, $deHallerCriterion_S$
for i in #Stages **do**
    if $i == 1$ **then**
        // Stage 1 Calculation
        Calculate ΔCw_1 using C_p, $\Delta T_{0S}[0]$, $\lambda[0]$, U
        Calculate $Cw1\_1$ and $Cw2\_1$
        Calculate β_1_1 and β_2_1
        Calculate α_1_1 and α_2_1
        Calculate $\Delta\beta\_1$
        Calculate de Haller criterion for rotor
        Calculate P_{03}/P_{01}, P_{03}, and T_{03}
        Calculate Λ_1
    else if $i == 2$ **then**
        // Stage 2 Calculation
        Set Λ_2 and update $\Delta T_{0S}[1]$
        Solve for β_1_2 and β_2_2
        Calculate α_1_2 and α_2_2
        Calculate $Cw1\_2$ and $Cw2\_2$
        Calculate ΔCw_2
        Calculate $\Delta\beta\_2$
        Calculate α_3_1
        Calculate de Haller criterion for rotor
        Calculate de Haller criterion for stator
        Calculate P_{03}/P_{01}, P_{03}, and T_{03}
    else
        // Stage Calculation for $i > 2$
        Set Λ_i and update $\Delta T_{0S}[i-1]$
        Solve for β_1_i and β_2_i
        Calculate α_1_i and α_2_i
        Calculate $Cw1\_i$ and $Cw2\_i$
        Calculate ΔCw_i
        Calculate $\Delta\beta\_i$
        Calculate α_3_i
        Calculate de Haller criterion for rotor
        Calculate de Haller criterion for stator
        Calculate P_{03}/P_{01}, P_{03}, and T_{03}

B. SIMULATION FIGURES

Algorithm 2. Root to Tip Calculations

Initialization of arrays for each stage data
    Declare and initialize arrays for stage parameters
for i **in** range#$Stages$ **do**
    if $i == 0$ **then**
        $r_r\_in\_rotor[i] \leftarrow r_r\_inlet$
        $r_t\_in\_rotor[i] \leftarrow r_t\_inlet$
    else
        $r_h\_in\_rotor[i] \leftarrow r_h\_out\_stator[i-1]$
        $r_t\_in\_rotor[i] \leftarrow r_t\_out\_stator[i-1]$
    Calculate $rm[i]$
    Calculate inlet rotor blade speeds:
        Calculate $U_r[i]$
        Calculate $U_m[i]$
        Calculate $U_t[i]$
    Calculate inlet rotor angles:
        Calculate $\beta_{1r}[i]$
        Calculate $\beta_{1m}[i]$
        Calculate $\beta_{1t}[i]$
    Calculate stator exit parameters:
        Calculate $C_3[i]$
        Calculate $T_3[i]$
        Calculate $P_3[i]$
        Calculate $\rho_3[i]$
        Calculate $A_3[i]$
        Calculate $h[i]$
        Calculate $r_t\_out\_stator[i]$
        Calculate $r_h\_out\_stator[i]$
    Calculate rotor outlet parameters:
        Calculate $r_t\_out\_rotor[i]$
        Calculate $r_h\_out\_rotor[i]$
        Calculate $U_t\_out\_rotor[i]$
        Calculate $U_r\_out\_rotor[i]$
    Calculate blade angles at rotor outlet:
        Calculate $Cw_{2r}[i]$
        Calculate $Cw_{2t}[i]$
        Calculate $\alpha_{2r}[i]$
        Calculate $\alpha_{2m}[i]$
        Calculate $\alpha_{2t}[i]$
        Calculate $\beta_{2r}[i]$
        Calculate $\beta_{2m}[i]$
        Calculate $\beta_{2t}[i]$
    Calculate relative flow angle change:
        Calculate $\Delta\beta_r[i]$
        Calculate $\Delta\beta_t[i]$
    Calculate degree of reaction:
        Calculate $^{\circ}\mathrm{R}_r[i]$

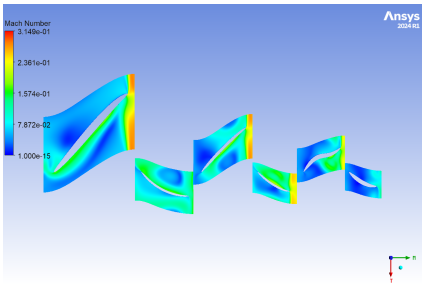

(a) Mach Number at 5000 RPM

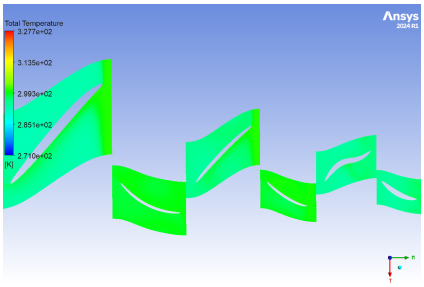

(b) Total Temperature at 5000 RPM

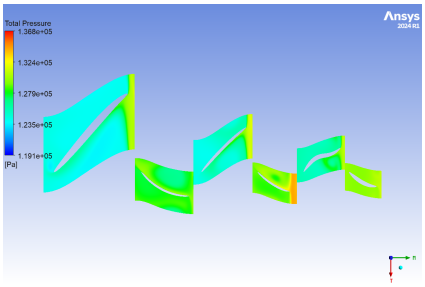

(c) Total Pressure at 5000 RPM

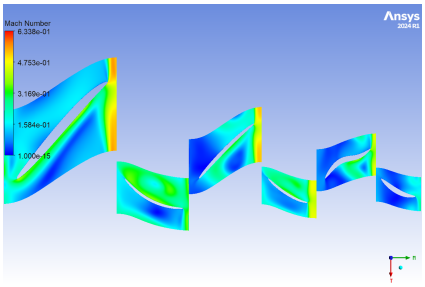

(d) Mach Number at 10000 RPM

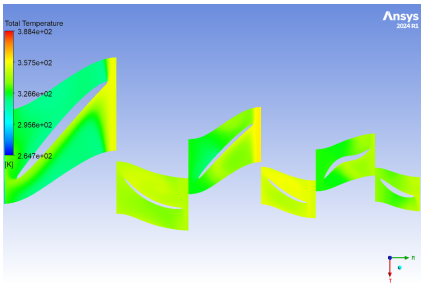

(e) Total Temperature at 10000 RPM

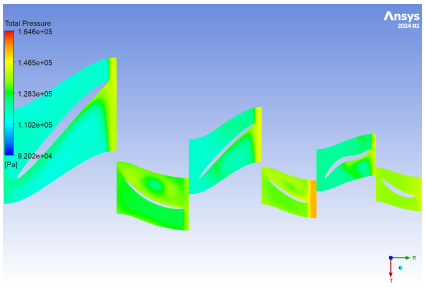

(f) Total Pressure at 10000 RPM

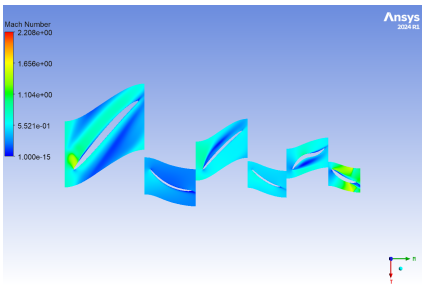

(g) Mach Number at 20600 RPM

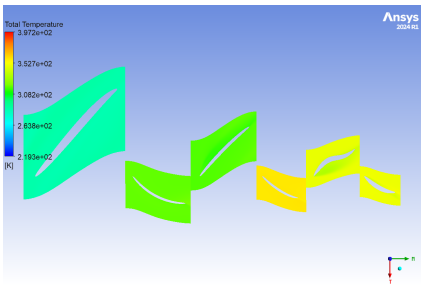

(h) Total Temperature at 20600 RPM

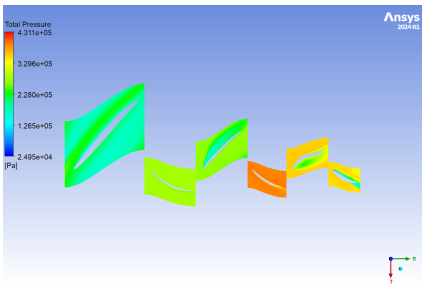

(i) Total Pressure at 20600 RPM

Fig. 4. Ansys Results for Different RPM Conditions